Visualization of Remote Sensing Imagery by Sequential Dimensionality Reduction on Graphics Processing Unit

Safa A. Najim[1,2] and Ik Soo Lim[1]
[1]*School of Computer Science, Bangor University, Bangor, Gwynedd, U.K.*
[2]*Computer Science Dept., Science College, Basrah University, Basrah, Iraq*

Keywords: Visualization, Dimensionality Reduction, Remote Sensing Imagery, Graphics Processing Unit (GPU).

Abstract: This paper introduces a new technique called *Sequential Dimensionality Reduction* (*SDR*), to visualize remote sensing imagery. The DR methods are introduced to project directly the high dimensional dataset into a low dimension space. Although they work very well when original dimensions are small, their visualizations are not efficient enough with large input dimensions. Unlike DR, *SDR* redefines the problem of DR as a sequence of multiple dimensionality reduction problems, each of which reduces the dimensionality by a small amount. The *SDR* can be considered as a generalized idea which can be applied to any method, and the stochastic proximity embedding (SPE) method is chosen in this paper because its speed and efficiency compared to other methods. The superiority of *SDR* over DR is demonstrated experimentally. Moreover, as most DR methods also employ DR ideas in their projection, the performance of *SDR* and 20 DR methods are compared, and the superiority of the proposed method in both correlation and stress is shown. Graphics processing unit (GPU) is the best way to speed up the *SDR* method, where the speed of execution has been increased by 74 times in comparison to when it was run on CPU.

1 INTRODUCTION

Visualization of high dimensional dataset is widely used in many fields including remote sensing imagery, biology, computer vision, and computer graphics in order to analyze them (Blum and Liu, 2006). The dimensionality reduction (DR) method is one of the best strategies used in this matter by projecting high dimensional space onto lower dimensional space where they can be visualized directly. The colour of each pixel in the visualization is a compendium of information in the original data in which their most salient features are captured (Kaski and Peltonen, 2011) (Peltonen, 2009).

Nonlinear projection has received significant attention in modern DR methods due to its intrinsic ability to generate visualization with respect to proximity between instances of data (Lawrence et al., 2011) (Mokbel et al., 2013). They have the advantage of perfect colours, which in turn often have clear meanings. In contrast, linear projection generates poor and worst interpretations of large datasets (Tyo et al., 2003) (Steyvers, 2002). The task of DR is visualization of neighbourhood or proximity relationships within a high dimensional space. The visualization should allow the user to retrieve the neighbouring data points in original space. Perfect neighbourhood preserving is usually not possible, and applying the DR method makes two kinds of errors: decreasing continuity neighbourhood, and increasing false neighbourhood (Lespinats and Aupetit, 2011). In false neighbourhoods, a large distance between original data points becomes a small distance in the lower dimensional space, which have the same colour in visualization, as in Figure 1. Thus, the colours of visualization have no meaning because the straightforward relationship with original high dimension space is lost (Bachmann et al., 2005).

Due to the difference between the topological structure of data points in high dimension space with the topological structure of projected space, it is difficult to preserve the neighbourhood relations between data points. Eventually, the way of applying DR itself is not perfect. Loss of any neighbour point could lead to an increase in the the amount of error because the missing neighbour point will occupy a place of another point in the lower space. Therefore, the amount of error could be growing explosively when increasing the false neighbourhood. Overlap between points is the dominate thing when direct projection

Najim S. and Lim I..
Visualization of Remote Sensing Imagery by Sequential Dimensionality Reduction on Graphics Processing Unit.
DOI: 10.5220/0004737500710079
In *Proceedings of the 5th International Conference on Information Visualization Theory and Applications* (IVAPP-2014), pages 71-79
ISBN: 978-989-758-005-5

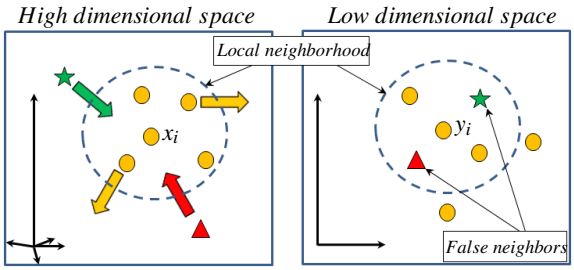

Figure 1: DR might cause the points which are outside local neighborhood in high dimension space to be inside local neighborhood in low dimension space. These points are called false neighborhood.

from high dimension space to lower dimension space is still used.

This work proposes a novel DR method, called *Sequential Dimensionality Reduction* (*SDR*), which is used to optimize the quality of visualization as a sequence of multiple dimensionality reduction problems, each of which reduces the dimensionality by a small amount. In contrast to the DR method, *SDR* preserves the neighbourhood relations between data points of two reduced consecutive spaces. Thus, false neighbourhoods are reduced as much as possible.

This paper is organized as follows: Section 2 gives some ideas about related works. In section 3, methodology of proposed method is explained. Experimental results are dominated in section 4. Finally, the conclusion is drawn in section 5.

2 RELATED WORK

2.1 Visualization by DR

The technique of DR is useful to visualize and analyse that large volume of data. For a set of n input points $X \in \Re^D$, $\phi(X)$ is used to project the D dimensional data points ($x_i \in X$) to d dimensional data points ($y_i \in Y$):

$$\phi : \Re^D \rightarrow \Re^d \quad (1)$$

$$x_i \mapsto y_i \;\; \forall \; 1 \leq i \leq n \quad (2)$$

In equation 1, ϕ attempts to approximate the input pairwise distance $r(x_i,x_j)$ with their corresponding in projected space $d(y_i,y_j)$, i.e, $r(x_i,x_j) \approx d(y_i,y_j) \;\; \forall \; 1 \leq i \leq n$ to project X's data point correctly in Y space. Loss of preserving neighborhood relations should be minimized, i.e. $\Xi(\phi(X)) \approx X$, where $\Xi : \Re^d \rightarrow \Re^D$. Thus, DR attempts to minimize Equation 3.

$$Stress(\phi) = \sum_{i,j=1}^{n} (r_{ij} - d_{ij})^2 \quad (3)$$

where $r_{ij} = ||x_i - x_j||$ and $d_{ij} = ||y_i - y_j||$.

The variety of strategies have resulted in the development of many different DR methods. Linear and nonlinear DR methods are the best examples to describe them.

Linear projection: Principle components analysis (PCA) uses orthogonal linear combination to find linear transformation space of data set. Because of its simplicity, it is used for data visualization (Jolliffe, 2002). Other visualization methods aim to preserve distances, such as multidimensional scaling (MDS) (Borg and Groenen, 1997). It computes distance matrix among points by computing pairwise Euclidean distances. PCA and MDS fail to find satisfactory low dimension representation of nonlinear data.

Nonlinear projection: Modern DR methods usually use nonlinear projections to project the data into low dimensions. Kernel PCA (Shawe-Taylor and Cristianini, 2004) is a nonlinear version of PCA, and isometric feature mapping (Isomap) (Tenenbaum et al., 2000) uses geodesic distance rather than Euclidean distance in MDS. Other methods use local linear relationships to measure the local structure, as in local linear embedding (LLE) (Roweis and Saul, 2000), maximum variance unfolding (MVU) preserves direct neighbours while unfolding data (Weinberger and Saul, 2006), and laplacian eigenmaps (Belkin and Niyogi, 2002) take a more principled technique by referring to the spectral properties of the resulting dissimilarity matrix. Some methods, like stochastic neighbor embedding (SNE) (Bunte et al., 2012), t-distributed stochastic neighbor embedding (t-SNE) (Maaten and Hinton, 2008) and neighborhood retrieval visualizer (NeRV) (Venna et al., 2010), attempt to match probability distributions induced by the pairwise data dissimilarities in the high dimensional space and low dimension space, respectively. Stochastic proximity embedding (SPE) proceeds by calculating Euclidean distance for global neighbourhood points within fixed radius (Agrafiotis et al., 2010). It is an enormous step in computational efficiency over MDS, and faster than Isomap.

Many solutions to visualize dataset in DR have been proposed (Maaten et al., 2009), but fewer solutions exist to overcome false neighbourhoods. The preserving neighbourhood relations by DR remains a matter of controversy between researchers.

2.2 Quality of Visualization

When measuring the quality of visualization for a given dataset it is important to know which DR method is best suited for the task at hand. Furthermore, humans cannot compare the quality of a given visualization with original data by visual inspection due to its high dimensionality. Thus, the best formal measurements should evaluate the amount of preserving neighbourhood colour distances in the visualization with their corresponding in original data. Correlation (ρ) and residual variance (RV) are the well-known methods used in this matter. If we suppose X is a vector of all pairwise distance of the data points in original space and Y is a vector of their corresponding pairwise colour distances in visualization, then their definitions are:

Residual Variance (RV) is a function used to compute the standard error of difference between visualization and original space (Tenenbaum et al., 2000). It calculates the sum of squares of differences between original data point distances and projected colour distances, as in equation 4.

$$RV = \sqrt{\frac{\sum(X-Y)^2}{N-2}} \tag{4}$$

where N is length of X vector. By Equation 4, small stress value indicates that visualization has very little error and higher efficiency.

In **Correlation function** (γ), the linear correlation between original input distances and colour distances in visualization is computed (Mignotte, 2012). The value of correlation is equal to 1 when all distances between two vectors are perfect preserved with positive slope. In the other hand, the value equal to -1 if the two vectors have prefect linear relationship with negative slope. The correlation is defined by:

$$\gamma = \frac{X^T\ Y/|X| - \overline{X}\ \overline{Y}}{\sigma_X\ \sigma_Y} \tag{5}$$

where $|X|$ is the length of X, and $\overline{X}$ and σ_X are the mean and standard deviation of X, respectively.

2.3 Visualization of Remote Scening Imagery

Remote scening imagery is a well-known technique to observe the earth and urban scenes by producing a large number of spectral bands (Smith, 2012). However, the challenge is how to display the abundant information contained in these images in a more interactive and easy analysed way, such as in a 3-D image cube. Due to the difficulty of using these huge bands, several DR methods are produced to overcome this problem by finding the best relationships among colour values in three colour channels after applying complex formulas to shrink the huge original space. DR provides a good way to visualize hyperspectral imagery by generating its colour image (Bachmann et al., 2005) (Mignotte, 2012).

2.4 Graphics Processing Unit (GPU)

Recently, the processing power and memory bandwidth of a new generation of graphics card have emerged as a powerful computation platform (Sanders and Kandrot, 2011). GPU has many programmable processors working in a highly parallel style. Compute Unified Device Architecture (CUDA) is the hardware and software NVIDIA parallel computing architecture that is Integrated Development Environment (IDE) such as Microsoft C++ Visual Studio, to write the CUDA C++ program. It has two types of functions: host and kernel. Host functions are run in CPU to execute the sequential codes, and kernel functions are responsible for the execution of the parallel instructions inside GPU. Kernel function cannot be called directly where it should be called from host function. The GPU consists of a set of small processing units (called threads) which are grouped into blocks. Each thread has a small private memory, and each block has memory to share their threads together. In addition, all GPU's threads can access CPU memory in a memory portion called global memory. Threads in a block synchronize their cooperation in accessing shared memory. Because the CPU consists of a few cores for executing serial processing, CPU and GPU construct a power combination which is designed for parallel and serial performances.

3 METHODOLOGY: SEQUENTIAL DR

The goal of the proposed method is to solve the DR by finding a representation of N points in d space, where its neighbourhood relationships are preserved with their corresponding relations in original space. To do that, we redefine the problem of DR as a sequence of multiple DR problems, each of which reduces the dimensionality by a small amount. We call this *Sequential Dimensionality Reduction* (*SDR*).

More specifically, given $X = x_1, x_2, ..., x_n$ be a data with instances $x_i \in \Re^D$. *SDR* attempts to do the

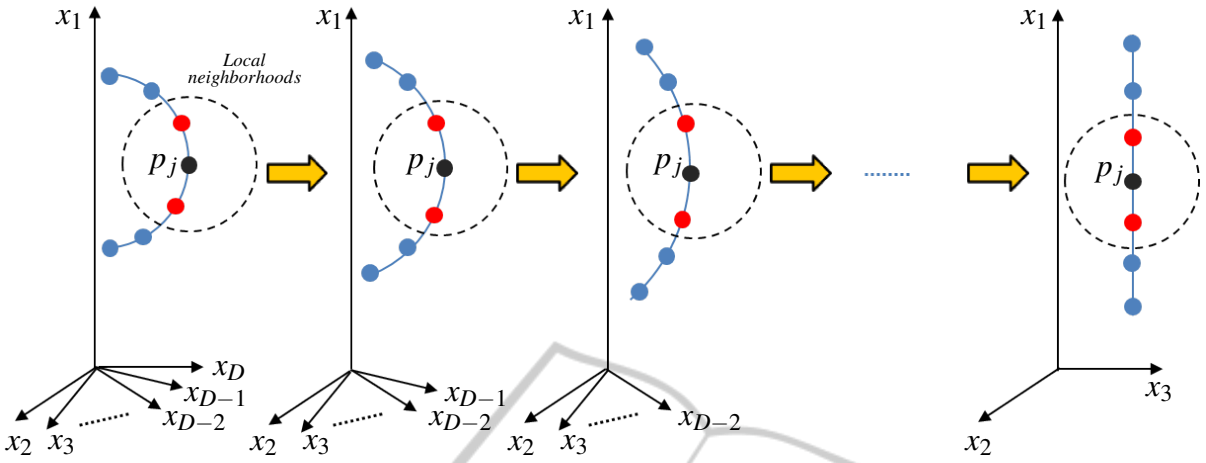

Figure 2: SDR redefines the problem of DR as a sequence of multiple DR problems, each of which reduces the dimensionality by a small amount. When amount of dimensionality reduction is equal to 1, the amount of losing information when transforming from v space to $v-1$ space is very few, where $v \in \{D, D-1, D-2, ..., d+1\}$. The neighborhoods of point p_j is preserved in $D-1$, $D-2$, ..., *and* d spaces.

transformation in equation 6.

$$G : \Re^D \xrightarrow{G_1} \Re^{D-1*S} \xrightarrow{G_2} \Re^{D-2*S} \xrightarrow{G_3} \Re^{D-3*S} .. \xrightarrow{G_k} \Re^d \quad (6)$$

where $D >> d$, and S is the step of dimensionality reduction can be in the range $[1,\ D-1]$.
The transformation (G_i) attempts to project N points of $(D-(i-1)*S)$ space into $(D-i*S)$ space. The transformation between two spaces is reasonably as close as possible because of the similarity of dimensionality between two spaces. Thus, the problem for $(D-i*S)$ space is solved. Efficiency of transformation permits to recursively apply it until the target dimension is obtained. Therefore, the neighbourhood relations between original points are kept carefully through a sequence of transformations until it obtains d space.

Figure 2 shows the general idea of the *SDR* when $S=1$. The point p_j in the v space is able to preserve its neighbour relationships when it is projected to the $v-1$ space. Thus, the amount of false neighbourhood when $G_v : \Re^v \rightarrow \Re^{v-1}$ is very small because the difference between the two spaces is just one dimension. A complete transformation from D space to d spaces is obtained by applying equation 6.

The point which should be discussed is how to choose S. As we defined before, S can be in the range $[1,\ D-1]$. For higher efficiency $S=1$, where the intermediate transformation problem will be between very close topology spaces. The error is minimized, and the problem is defined as a $D-1$ DR problem. The efficiency is reduced when $S>1$, and the worst case when $S=D-1$ which is defined as one DR problem.

SDR accepts as input set of N points in D space, a transformation function G, and the amount of dimensionality reduction S. d is the dimension of lower space which should be given. *SDR* algorithm recursively reduces the dimensionality of a space until obtaining the target space, and the following steps describe that:

1. let $v = D$.
2. if v is equal to d {Stop}
3. let $v-S$ is the dimension of the next lower space.
4. N points of v space is projected in $v-S$ space by applying $G : \Re^v \rightarrow \Re^{v-S}$.
5. let $v = v-S$, and go to step 2.

Briefly, *SDR* put the projected points in the correct location in low dimension space, which leads to a reduction in the amount of error and an increase in the degree of compliance with original space. The efficiency of *SDR* is clearer when input dimension is very high and target dimension is very low. We chose the SPE method to be used with the *SDR* idea (to generate *SSPE*) because SPE has more advantages than other methods, as we will see in next subsection.

The length of the execution time is one of the limitations that is encountered with the *SDR*, therefore, using GPU is the most appropriate way to overcome this problem.

3.1 SPE

SPE is a nonlinear method and proceeds by calculating Euclidean distance for global neighbourhood

points within a fixed radius (r_c) (Agrafiotis et al., 2010). SPE is an enormous step forward in computational efficiency over MDS, and faster than Isomap. SPE is used in different applications and has succeeded in getting satisfactory results (Ameer and Jacob, 2012). The objective of SPE is to find a representation which has point's distances which are identical to their corresponding distances in high dimensional space. The method starts by selecting a random point from the original data, in time (t_k) to be projected in the low dimension space. Projection points means the withdrawal of the neighbourhood points within fixed radius (r_c).

Projected space starts with initial coordinates, and it is updated iteratively by placing y_j onto the projected space in such a way that their euclidean distance ($d_{ij} = ||y_i - y_j||$) is closed to the corresponding distance ($r_{ij} = ||x_i - x_j||$) in original high dimensions space. Thus, SPE minimizes Equation 3. The points in projected space are updated according to following constraint:

$$if(r_{ij} \leq r_c)\ or\ ((r_{ij} > r_c)\ and\ (d_{ij} < r_{ij}))$$

$$x_j \leftarrow x_j + \lambda(t_k)\frac{r_{ij} - d_{ij}}{d_{ij} + \varepsilon} \quad (7)$$

where $\lambda(t_k)$ is learning rate at t_k time, and ε a tiny number used to avoid division by zero (we used $\varepsilon = 1\text{x}10^{-8}$.

SDR with SPE generates a new method, which we call *SSPE*, which uses the idea of *SDR* and SPE's objective function. While SPE objective function is proved by its minimized function (Agrafiotis et al., 2010) when transforming D space to d space ($D >> d$), *SSPE* will be minimizing for the same reasons because nothing is changed in relation between D and d spaces.

4 EXPERIMENTAL RESULTS

In this section, the *SDR* and DR methods are evaluated in quantitative and qualitative manners. The performance of the proposed method is analysed using remote sensing imagery dataset. The *SDR* idea is implemented on SPE, which is called *SSPE*, and compared with tradition SPE. The comparison *SDR* with 20 DR methods is also included, and Table 1 shows information about those methods.

The implementations were carried out on a computer which has Intel(R) Cores(TM) i5 CPU M520 2.4Ghz and NVIDIA GeForce GTX 280 with buffer size 1024 MBytes. Matlab and Microsoft Visual Studio C++ 2008 Professional Edition with CUDA were used to write the codes. We used the AVIRIS Moffet Field data set from the southern end of San Francisco Bay, California, done in 1997 (AVIRIS, 2013). Because some methods cannot work with large dataset, we divided this dataset into small regions, each one with 300x300x224 pixels, and we selected 3 regions of them.

Table 1: Methods employed in comparison. The first column contains the name of methods, second column shows the type (T) of method (linear (L) or nonlinear (NL)), third column shows the source of reference and the symbol ✓ in the fourth column indicates the original codes (O) have been used.

Method	T	Source	O
PCA	L	(Jolliffe, 2002)	✓
CCA	L	(Demartines and Hrault, 1997)	
CDA	NL	(Lee et al., 2004)	✓
Factor_analysis	NL	(Darlington, 1999)	
Fast_MVU	NL	(Weinberger and Saul, 2006)	
Hessian_LLE	NL	(Donoho and Grimes, 2005)	
Isomap	NL	(Tenenbaum et al., 2000)	✓
Kernel_PCA	NL	(Shawe-Taylor and Cristianini, 2004)	
Laplacian	NL	(Belkin and Niyogi, 2002)	
LDA	L	(Duda et al., 2001)	
LLC	NL	(Shi and Malik, 2000)	
LLE	NL	(Roweis and Saul, 2000)	✓
LLTSA	NL	(Zhang et al., 2007)	
LPP	L	(Zhi and Ruan, 2008)	
LTSA	NL	(Zhang and Zha, 2004)	
NPE	NL	(He et al., 2005)	✓
Prob_PCA	NL	(Tipping and Bishop, 1999)	
SPE	NL	(Agrafiotis et al., 2010)	✓
SNE	NL	(Bunte et al., 2012)	✓
tSNE	NL	(Maaten and Hinton, 2008)	✓

Table 2 shows *SSPE* achieves more accurate correlation and stress values. For all regions, the correlation values by our proposed method are highest, and same is also true for stress values in which it has given lesser values.

To compare the *SDR* and DR methods in a qualitative manner, the visualizations of SPE and *SSPE* are compared, as in the Figure 3. The performances of the proposed method in previous table are conformed here. For example, in the visualizations of regions 1, 2, and 3, *SSPE*s' visualizations show more details,

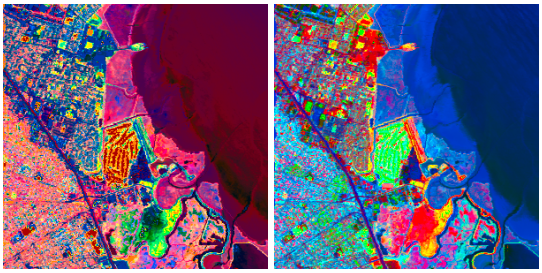

(a) R_1

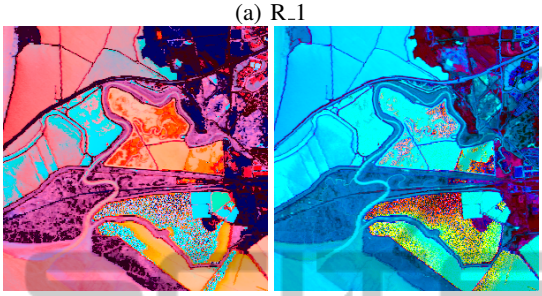

(b) R_2

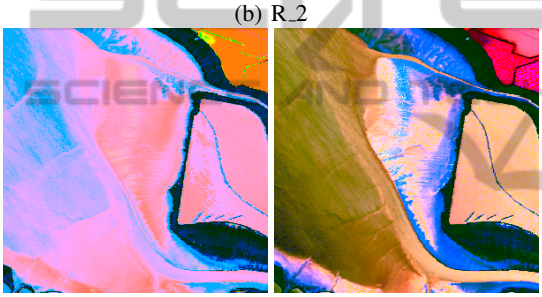

(c) R_3

Figure 3: Visualizations of regions 1, 2, and 3 by using SPE (in left side) and SSPE (on the right side). The SSPE's visualizations in all regions show more details than SPE's visualizations.

Table 2: Results of comparison the *SDR* method (represented by *SSPE*), when $S = 1$, with the DR method (represented by SPE). The proposed method got the highest correlation and less stress values in all regions.

	Correlation		Stress	
	SPE	SSPE	SPE	SSPE
R_1	0.696	0.998	0.033	0.022
R_2	0.641	0.966	1.504	0.261
R_3	0.813	0.989	1.102	0.131

which cannot be recognized by SPE. Let us explain that with this example, in the top right corner of the visualization of region 3, the area is incorrectly visualized by SPE, but it has been well visualized by *SSPE*. This is due to the fact the number of false colours are higher than true colours in SPE's visualization, which effected the accuracy of that area. The same situation occurs in the remaining regions where the proposed method was proven to show the correct colours.

The results of comparisons of the proposed method with 20 DR methods for regions 1, 2 and 3 are shown in Table 3, and Figure 4 shows the visualizations of region 1 by these methods. The results confirmed and supported our aforementioned discussion about efficiency of the proposed method. Although SPE is not the best among the other methods, *SSPE* is much better than them in correlation and stress measurement values. Figure 5 shows the highest correlation and less stress measurement values, of average values in Table 3, are got by *SSPE*.

Table 3: Correlation and stress values of comparisons among 21 methods for three regions. *SSPE* , when $S = 1$, is the best in all cases, where it has higher correlation and lesser stress values than other methods.

	Correlation			Stress		
Method	R_1	R_2	R_3	R_1	R_2	R_3
PCA	0.69	0.67	0.70	0.71	1.37	4.30
CCA	0.86	0.52	0.53	0.11	1.27	0.97
CDA	0.55	0.75	0.75	5.70	1.18	2.21
Fact_analysis	0.83	0.42	0.65	0.90	3.88	0.32
Fast_MVU	0.34	0.40	0.00	3.50	5.68	3.03
Hessian_LLE	0.27	0.29	0.00	0.72	5.43	2.13
Isomap	0.53	0.65	0.45	0.72	1.13	1.44
Kernel_PCA	0.70	0.77	0.59	0.44	0.96	0.46
Laplacian	0.24	0.62	0.58	1.08	1.77	0.97
LDA	0.26	0.43	0.59	1.86	1.04	5.53
LLC	0.24	0.34	0.32	2.42	1.84	3.52
LLE	0.33	0.37	0.37	0.71	1.45	2.86
LLTSA	0.32	0.43	0.21	1.08	1.75	0.97
LPP	0.75	0.61	0.66	1.12	1.78	0.97
LTSA	0.28	0.28	0.22	1.12	1.61	0.97
NPE	0.40	0.31	0.33	1.08	1.75	0.94
Prob_PCA	0.47	0.64	0.72	0.76	1.30	1.80
SPE	0.69	0.64	0.81	0.03	1.50	1.10
SNE	0.40	0.64	0.73	2.56	1.56	1.23
tSNE	0.58	0.44	0.65	3.87	1.18	2.56
SSPE	**0.99**	**0.96**	**0.98**	**0.02**	**0.26**	**0.13**

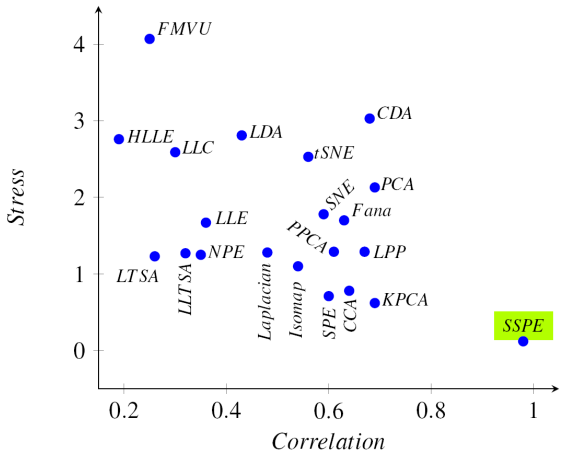

Figure 5: The average of comparisons, in the Table 3, the SSPE and 21 methods, SSPE is the best for getting the highest correlation and the least stress values, which are 0.98 and 0.14, respectively.

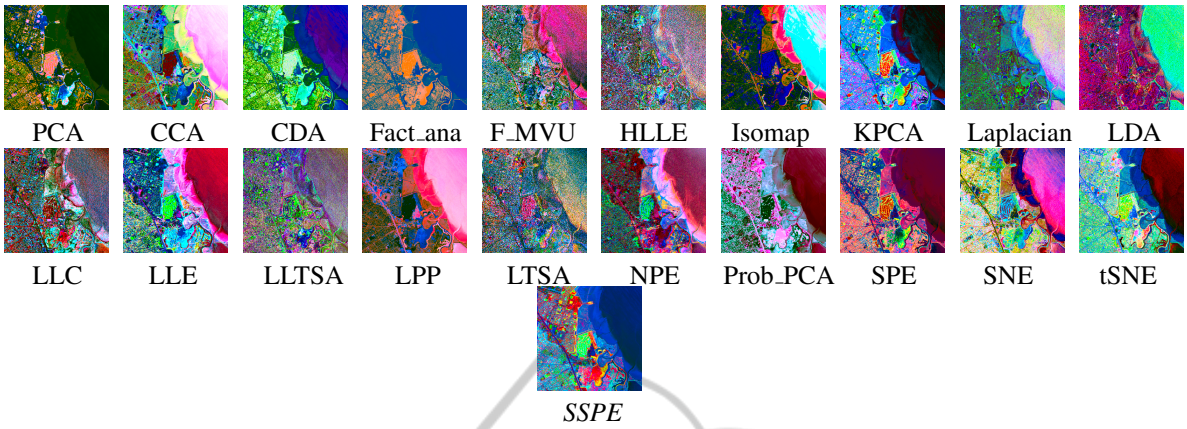

Figure 4: Visualization of region 1 by using 21 DR methods. According to the Table 3, the worst visualization is got by Laplacian method, and SSPE's visualization is the best visualization among them.

The speed is the next important item which should be addressed. The DR idea is much faster than our proposed method. Thus, GPU is the best way to speed up the *SDR* method, that is, where the speed of execution has been increased by 74 times than when it ran on CPU, as in the Figure 6. Thus, the speed problem that occurs in *SDR* is solved. Interestingly, the consumed time by the proposed method is important where the error is gradually lessened until it reaches to be up to less than what can be. Figure 7 shows the efficiency of the DR method (represented by SPE) is not affected by increasing the iteration number.

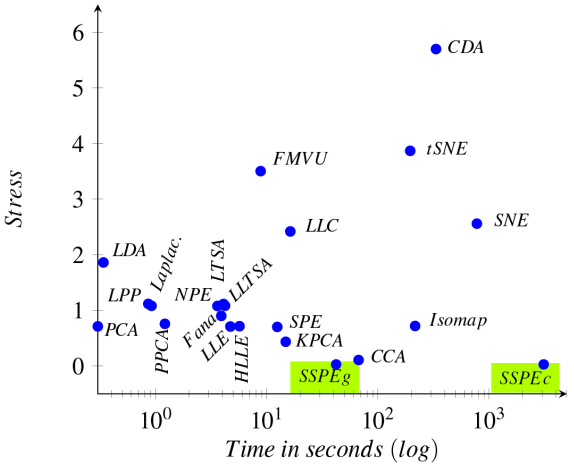

Figure 6: The role of using GPU was very positive to increase the speed of proposed method (SSPE) from 3107.147 seconds in CPU (which is called $SSPE_c$) to 42.049 seconds in GPU (which is called $SSPE_g$). Thus, the execution speed of SDR is acceptable when comparing that with those of other methods.

Even though our method gave good results when the sequences of multiple dimensionality reduction

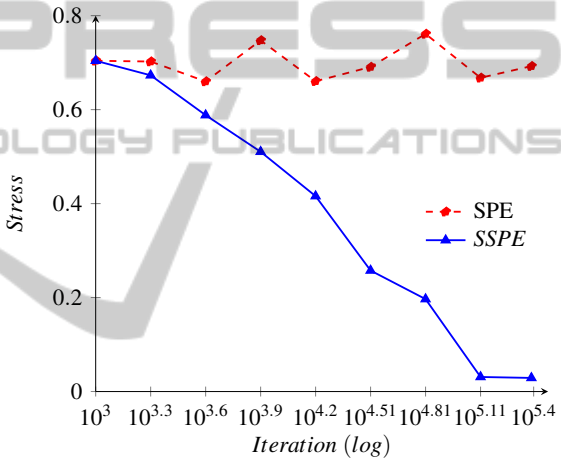

Figure 7: SPE and SSPE use the same number of iterations. In SPE, there is no significant impact on the change in SPE's efficiency through iterations, but the stress is reduced gradually with SSPE.

are reduced by amount equal to one, this amount can be larger than one. However, the efficiency of *SDR* is reduced when S is increased, as in Figure 8.

5 CONCLUSIONS

A new method called *SDR* has been proposed in this paper to visualize remote sensing imagery. Theoretically, we illustrated that *SDR* maintains and preserves the relations among neighbour points in low dimensionality space. The results showed the accuracy of the proposed *SDR* which leads to a better visualization with minimum false colours compared to the direct projection of DR method, where those results were confirmed by comparisons of our method with 20 other methods. It has been also demonstrated that

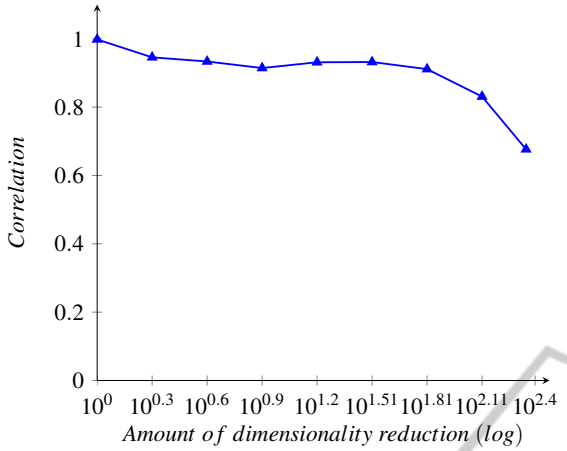

Figure 8: The correlation measurement value of SDR is very high (which is equal to 0.998) when the amount of dimensionality reduction is equal to 1. The efficiency of SDR is reduced when this reduction amount is greater than 1, and the lowest correlation value is (0.676) when reduction amount is equal to 223.

the speed of *SDR* on GPU is much faster than it is on CPU.

ACKNOWLEDGEMENTS

It would not have been possible to write this paper without the help and support of the Ministry of Higher Eduction and Scientific Research in Iraq. The authors would like to acknowledge the financial and academic support of the Basrah and Bangor Universities.

REFERENCES

Agrafiotis, D. K., Xu, H., Zhu, F., Bandyopadhyay, D., and Liu, P. (2010). Stochastic proximity embedding: Methods and applications. *Molecular Informatics*, 29:758–770.

Ameer, P. M. and Jacob, L. (2012). Localization using stochastic proximity embedding for underwater acoustic sensor networks. In *2012 National Conference on Communications (NCC)*.

AVIRIS (2013). *http://aviris.jpl.nasa.gov/index.html*.

Bachmann, C. M., Ainsworth, T. L., and Fusina, R. A. (2005). Exploiting manifold geometry in hyperspectral imagery. *IEEE transaction on geoscience and remote sensing*, 43:441–454.

Belkin, M. and Niyogi, P. (2002). Laplacian eigenmaps and spectral techniques for embedding and clustering. *Advances in Neural Information Processing Systems*, 14:585591.

Blum, R. S. and Liu, Z. (2006). *Multi-sensor Image Fusion and its Applications*. Taylor & Francis Group.

Borg, I. and Groenen, P. J. (1997). *Modern Multidimensional Scaling : Theory and Applications*. Springer-Verlag, NewYork.

Bunte, K., Haase, S., Biehl, M., and Villmann, T. (2012). Stochastic neighbor embedding (sne) for dimension reduction and visualization using arbitrary divergences. *Neurocomputing*, 90:23–45.

Darlington, R. B. (1999). Factor analysis. Technical report, Cornell University,.

Demartines, P. and Hrault, J. (1997). Curvilinear component analysis: a self-organizing neural network for nonlinear mapping of data sets. *IEEE Transactions on Neural Networks*, 8:148–154.

Donoho, D. L. and Grimes, C. (2005). Hessian eigenmaps: New locally linear embedding techniques for high-dimensional data. In *The National Academy of Sciences, 102(21):74267431.*

Duda, R. O., Hart, P. E., and Stork, D. G. (2001). *Pattern Classification*. Wiley Interscience Inc.

He, X., Cai, D., Yan, S., and Zhang, H.-J. (2005). Neighborhood preserving embedding. In *Tenth IEEE International Conference on Computer Vision (ICCV) (Volume:2)*.

Jolliffe, I. (2002). *Principal Component Analysis*. Springer Verlag, New York, Inc.

Kaski, S. and Peltonen, J. (2011). Dimensionality reduction for data visualization. *IEEE signal processing magazine*, 28:100–104.

Lawrence, J., Arietta, S., Kazhdan, M., Lepage, D., and OHagan, C. (2011). A user-assisted approach to visualizing multidimensional images. *IEEE Transaction on Visualization and Computer Graphics*, 17(10):1487–1498.

Lee, J. A., Lendasse, A., and Verleysen, M. (2004). Nonlinear projection with curvilinear distances: Isomap versus curvilinear distance analysis. *Neurocomputing*, 57:49–76.

Lespinats, S. and Aupetit, M. (2011). Checkviz: Sanity check and topological clues for linear and non-linear mappings. *Comput. Graph. Forum*, 30:113–125.

Maaten, L. V. D. and Hinton, G. (2008). Visualizing data using t-sne. *Machine Learning Research*, 9:2579–2605.

Maaten, L. V. D., Postma, E., and Herik, H. V. D. (2009). Dimensionality reduction: A comparative review. *Machine Learning Research*, 10:1–41.

Mignotte, M. (2012). A bicriteria-optimization-approach-based dimensionality-reduction model for the color display of hyperspectral images. *IEEE Transactions on Geoscience and Remote Sensing*, 50:501–513.

Mokbel, B., Lueks, W., Gisbrecht, A., and Hammera, B. (2013). Visualizing the quality of dimensionality reduction. *Neuocomputing*, 112:109–123.

Peltonen, J. (2009). Visualization by linear projections as information retrieval. *Advances in Self-Organizing Maps Lecture Notes in Computer Scienc*, 5629:237–245.

Roweis, S. T. and Saul, L. K. (2000). Nonlinear dimensionality reduction by locally linear embedding. *science*, 290:2323–2326.

Sanders, J. and Kandrot, E. (2011). *CUDA by example*. Addison-Wesley Professional.

Shawe-Taylor, J. and Cristianini, N. (2004). Kernel methods for pattern analysis. *Cambridge University Press*.

Shi, J. and Malik, J. (2000). Normalized cuts and image segmentation. *IEEE Transaction on Pattern Analysis and Machine Intelligence*, 22:888–905.

Smith, R. B. (2012). *Introduction to Hyperspectral Imaging*. MicroImages, Inc.

Steyvers, M. (2002). Multidimensional scaling. *Encyclopedia of Cognitive Science*.

Tenenbaum, J. B., de Silva, V., and Langford, J. C. (2000). A global geometric framework for nonlinear dimensionality reduction. *Science 290*, 5500:2319–2323.

Tipping, M. E. and Bishop, C. M. (1999). Mixtures of probabilistic principal component analyzers. *Neural Computation*, 61:611.

Tyo, J. S., Konsolakis, A., Diersen, D. I., and Olsen, R. C. (2003). Principal-components-based display strategy for spectral imagery. *IEEE transactions on geoscience and remote sensing*, 41:708718.

Venna, J., Peltonen, J., Nybo, K., Aidos, H., and Kaski, S. (2010). Information retrieval perspective to nonlinear dimensionality reduction for data visualization. *J. Mach. Learn. Res*, 11:451–490.

Weinberger, K. Q. and Saul, L. K. (2006). An introduction to nonlinear dimensionality reduction by maximum variance unfolding. In *Proceedings of the National Conference on Artificial Intelligence, Boston, MA*.

Zhang, T., Yang, J., Zhao, D., and Ge, X. (2007). Linear local tangent space alignment and application to face recognition. *Neurocomputing*, 70:1547–1553.

Zhang, Z. and Zha, H. (2004). Principal manifolds and nonlinear dimensionality reduction via local tangent space alignment. *SIAM Journal of Scientific Computing*, 26:313–338.

Zhi, R. and Ruan, Q. (2008). Fractional supervised orthogonal local linear projection. In *CISP '08. Congress on (Volume:2) Image and Signal Processing.*